Drying Biomass Using Waste Heat from Biomass Ash by Means of Heat Carrier

Gang Li, Zilin Li, Taikun Yin, Jingpin Ren, Yalei Wang, Youzhou Jiao, and Chao He *

Agricultural and forestry biomass direct-fired power generation represents an important technology to promote low-carbon energy transition and sustainable development. To solve the problems of boiler output fluctuation caused by unstable combustion of high moisture content biomass and insufficient recovery of ash waste heat after combustion, steel heat carriers (HC) were used to absorb high-temperature ash (HTA) waste heat, and then HC was directly mixed with high moisture biomass for dewatering and drying. The thermal efficiency of waste heat recovery decreased with the increase of ash temperature, and the highest thermal efficiency of waste heat recovery was 77.4% at a heat-carrying spheres temperature (THC) of 600 °C and a mixing mass ratio of 3. Through the optimization of waste heat recovery and mixed drying process, at a biomass ash temperature of 800°C, 1 kg of ash was able to dry 0.75 kg of high moisture content biomass, resulting in a reduction in fuel moisture by about 10%.

DOI: 10.15376/biores.17.3.5243-5254

Keywords: Biomass drying; Heat carrier; Biomass ash; Waste heat utilization

Contact information: College of Mechanical and Electrical Engineering, Henan Agricultural University, Henan Province, 450002, China; Key Laboratory of New Materials and Facilities for Rural Renewable Energy; Ministry of Agriculture, Zhengzhou, Henan Province, 450002, China; Henan Province Rural Renewable Energy Key Laboratory, Zhengzhou, Henan Province, 450002, China; Collaborative Innovation Center of Biomass Energy; Zhengzhou, Henan Province, 450002, China;
** Corresponding author: hechao666777@163.com*

INTRODUCTION

The current over-consumption of fossil energy sources has caused severe climate problems. The utilization of clean energy such as biomass has become a research hot spot (Favero *et al*. 2020; Xing *et al*. 2021). Biomass fuels account for approximately 11% of global energy consumption (Agar *et al*. 2020), and during the period from January to June 2021, China generated 77.95 billion kWh of electricity from biomass, an increase of approximately 26.6% year-on-year (NEA 2021). Forestry and agricultural wastes usually have a base moisture content between 30% and 60% due to their own hygroscopicity and transportation and storage conditions (Fagernäs *et al*. 2010). High moisture biomass and carried dust can cause delayed ignition (Shanmukharadhya and Sudhakar 2007) and combustion control problems in boilers (Smith *et al*. 2013). Because drying biomass improves fuel quality and boiler operational stability, biomass is usually pretreated by drying before combustion. Currently, biomass power plant fuels are dried by natural ventilation (Li *et al*. 2011). Natural ventilation drying has a long storage cycle, takes up a lot of space, and produces gases that pollute the atmosphere by accumulating and rotting over a long period of time (Rupar *et al*. 2003).

An important goal in the development of a drying process is to minimize the overall operational cost of the process. Drying fuels using waste heat from biomass power plants as the thermal source can reduce drying costs. At present, many scholars have worked on high temperature flue gas waste heat drying biomass. Bioenergi AB company dried sawdust with boiler flue gas at 300 °C with an evaporation capacity of approximately 6 to 7 tons/hour and an outlet air temperature of 105 to 200 °C(Salomonsson *et al*. 2006). Holmberg (2007) built a small, fixed bed dryer using secondary flue gas at 70 to 120 °C with a minimum energy consumption of 2.7 MJ/Kg. The high humidity of boiler flue gas is not suitable for direct fuel drying, and the high outlet air temperature requires the configuration of subsequent devices to recover waste heat to improve the energy efficiency of drying (Amos 1998). The annual generation of biomass ash is approximately 47,500 tons (Munawar *et al*. 2021). Biomass ash is generally discharged at 650 to 800 °C (Wei *et al*. 2017) and is stable in yield and form, making it an available high-temperature resource. This study explored a low-cost ash residue waste heat recovery system for efficient drying of biomass fuels to improve the thermal efficiency and equipment operational stability of biomass power plants.

An important accomplishment of the present work is the fact that the steel balls can be separated from the mixture with ash. Many scholars have studied the chemical and thermophysical properties of the residue after combustion or pyrolysis of the material. Sunil *et al.* (2020) analyzed the chemical composition and crystallization of biomass residue and found that its main oxides are silica, calcium oxide, magnesium oxide, *etc*., and at that the crystallized substances include silicates such as calcium feldspar. Seebold (2017) analyzed the slag after biomass pyrolysis and determined that its specific heat capacity was from 0.8 to 1.6 J/(Kg•°C) using the sapphire method (ASTM E-1269-2011), with a glass transition at 600 °C. Most biomass power plants use the water quenching method to treat HTA, and some scholars have studied the waste heat recovery of metallurgical slag (Seebold *et al*. 2017). Jahanshahi *et al.* (2011) designed a moving bed heat exchanger to recover waste heat from steel slag (1200 °C), where the outlet temperature of hot air is 500 to 600 °C. Junxiang *et al*. (2015) used water as the heat transfer medium to recover (300 to 700 °C) slag waste heat by a tubular heat exchanger to obtain more than 55% waste heat recovery efficiency with a much lower temperature outlet slag. In the process of waste heat recovery from biomass ash slag by heat carriers, the waste heat recovery thermal efficiency and the temperature of heat carrier (HC) are important evaluation criteria, and the best $MR_{HC/HTA}$ and D_{HC} need to be explored in the experiment. In the study of direct mixing of HC with biomass fuel for drying, the diameter of HC, the T_{HC}, and the $MR_{HC/HTA}$ are important factors affecting the drying process, and the drying thermal efficiency (average evaporation energy consumption) and the extent of fuel dehydration are important evaluation criteria.

In response to the status of waste heat utilization of high moisture fuels from biomass power plant ash, the use of steel HC to recover waste heat from HTA, which is then used to mix and dry high moisture biomass fuels, provides a technical reference for waste heat recovery and utilization of similar HTA.

EXPERIMENTAL

Materials

Biomass ash was received from the Henan Hengguang biomass power plant. Peanut shells were taken from the suburbs of Zhengzhou, Henan Province, with a length of 2 to 4 cm and manually adjusted moisture content. The HC were made of 304 stainless steel with thermophysical properties as shown in Table 1, with diameters of 6, 9, 12, 15, and 18 mm. The collected biomass ash was crushed, ground, and passed through a 120-mesh sieve. The metal oxides were analyzed by Malvern PANalytical Zetium X-ray fluorescence spectrometer (XRF; Almelo, Netherlands). A Rigaku MiniFlex 600 X-ray diffractometer (XRD; Osaka, Japan) was used to analyze the crystal structure. The composition of biomass ash oxides is shown in Table 2. Results of crystallographic analysis are shown in Fig 1.

Table 1. Specific Heat of HC (Das *et al.* 2007)

Temperature (°C)	25	100	200	300	400	500	600	700	800
Specific heat J/(Kg•°C)	0.48	0.5	0.53	0.54	0.56	0.57	0.595	0.6	0.62

Table 2. XRF Analysis of Biomass Ash

Ingredients	SiO_2	CaO	Fe_2O_3	Al_2O_3	K_2O	MgO	Na_2O	TiO_2	others
Quality (%)	40.37	23.25	11.85	9.70	4.17	4.06	1.92	1.13	3.55

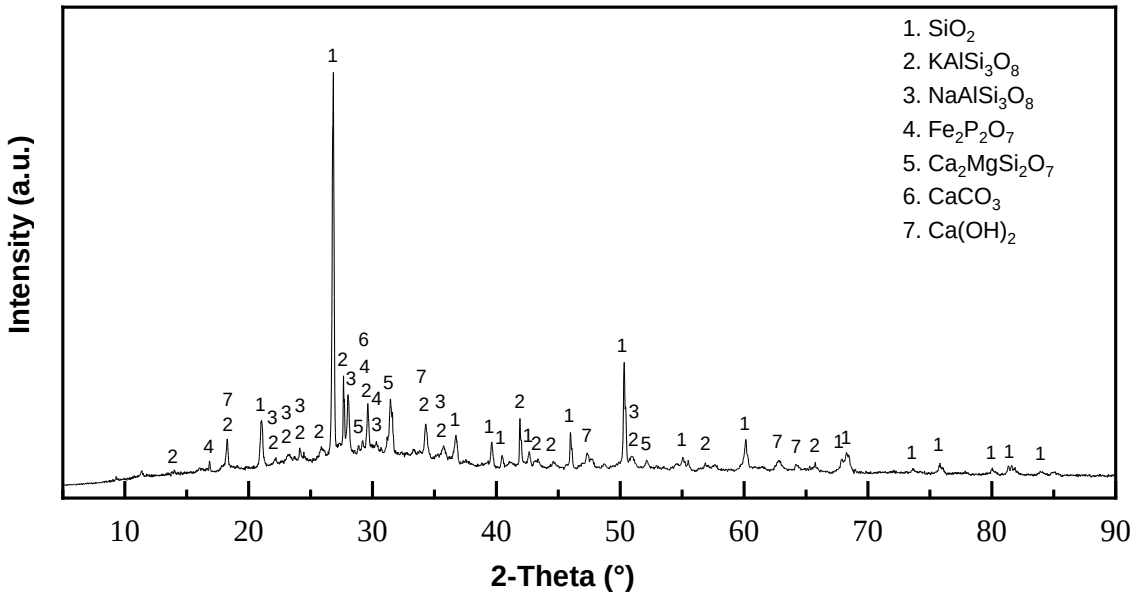

Fig. 1. XRF analysis of biomass ash

Device and Methods

The main structure of the mixing and drying device is 304 stainless steel. The outer surface is covered with aluminum silicate fiber insulation layer. The mixing and drying device is a total of 3 layers, and the layer height is 25 cm. The staggered material drop port is set between the layers, and the mixing speed of the material and the heat carriers is adjusted by a frequency conversion motor. The structure of the device is shown in Fig. 2.

To determine the thermophysical properties, biomass ash was analyzed by TG-DSC with TA instruments SDT650 simultaneous thermal analyzer (New Castle, DE, USA), and the specific heat of biomass ash was tested by the DSC sapphire method. Due to the complex composition of biomass ash, platinum crucibles were chosen to obtain better thermal analysis test results at high temperatures. The protective gas was nitrogen with an airflow rate was 50 mL/min, and the heating rate was 20 °C/min.

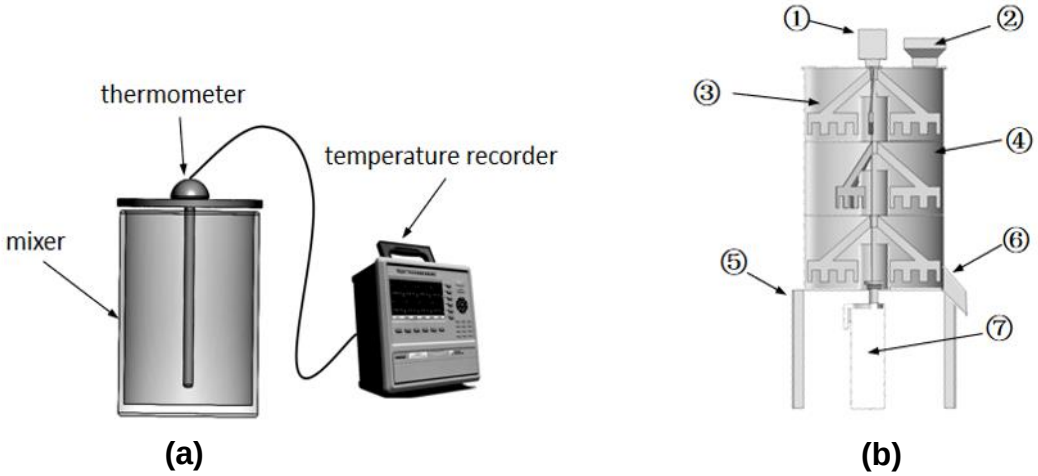

Fig. 2. (a) Waste heat recovery device diagram. (b) Mixing and drying test device diagram: (1) Exhaust gas cooling; (2) Inlet; (3) Stirring sheet; (4) Cavity; (5) Brackets; (6) Discharge port; (7) Speed control motor

The D_{HC} affects the heat transfer surface area and the material contact area and frequency. The heat storage capacity of the waste heat recovery product carrier sphere is influenced by the temperature of biomass ash, the size of the carrier sphere, the mixing ratio of the carrier sphere and biomass ash, and the insulation performance of the mixed heat exchanger. To reduce the heat loss in the heat exchange process, the mixed drying device adopted a double-layer design, and the test used different D_{HC} and $MR_{HC/HTA}$ to recovery waste heat of different T_{HTA}. The slag temperature in the furnace of biomass power plants is generally above 600 °C (Wei *et al*. 2017). To examine the heat exchange between ash slag and HC, biomass ash slag was placed in muffle furnace and heated to 600, 700, 800, 900, and 1000 °C, and a constant temperature was maintained for 5 min. The HTA and HC (D_{HC} =12 mm) in mass ratios of 1:1.5, 1:2, 1:2.5, 1:3 and 1:3.5 were put into the waste heat recovery device, and the temperature was recorded. And then 600 g of biomass ash was heated to 800 °C in the furnace, mixed with 900 g of particles of sizes 6, 9, 12, 15, and 18 mm HC, and the temperature was recorded. Then use a screen to separate the heat carrier balls.

The mixing and drying of biomass with HC was performed as follows. The HC in the muffle furnace was heated to 300, 350, 400, 450, or 500 °C and maintained at a constant temperature for 5 min. The biomass was added into the mixing and drying device first, and the drop gate was closed. After the speed control motor was turned on, high temperature HC and biomass fuel was added and mixed quickly for 5 min. The temperature change during the mixing process of HC and material was measured with infrared temperature measuring gun, and then it was discharged from the discharge port. Electromagnet was used to separate heat carrier ball and peanut shells.

Biomass moisture was determined according to GB/T 28733 (2012).

Equations

The biomass ash specific heat was calculated by Eq. 1,

$$C_{sp} = \frac{DSC_{sp} - DSC_{base}}{DSC_{sd} - DSC_{base}} \times \frac{m_{sd}}{m_{sp}} \times C_{sd} \quad (1)$$

where C_{sp} is specific heat of biomass ash (j·g-^{1}·℃$^{-1}$), C_{sd} is specific heat capacity of sapphire (j·g-^{1}·℃$^{-1}$), DSC_{sp} is DSC signal of the sample (mv), DSC_{sd} is DSC signal of the sapphire (mv), and DSC_{base} is base line (mv).

The biomass fuel dehydration was calculated by Eq. 2,

$$x = w_1 - w_2 \quad (2)$$

where w_1 is moisture content before drying (%), w_2 is moisture content after drying (%), and x is biomass fuel dehydration percentage (%).

The thermal efficiency of waste heat recovery was calculated by Eq. 3,

$$y = \frac{(t-t')c_1'}{(T-t)c_2'} \times 100\% \quad (3)$$

where c_1' is specific heat of heat carriers (j·g-^{1}·℃$^{-1}$), c_2' is specific heat of biomass ash (j·g-^{1}·℃$^{-1}$), T is Pre-mixing temperature of ash (℃), t is temperature after mixing HC/ash temperature (℃), and t' is temperature of the air (℃).

The drying thermal efficiency was calculated by Eq. 4,

$$\eta' = \frac{xm_2e'}{(t_1-t_2)c_1m_1} \quad (4)$$

where e′ is latent heat of water vaporization (j/g), m_1 is mass of HC (g), m_2 is fuel mass before mixing and drying(g), C_1 is specific heat capacity of heat carriers (j/(g·℃)) (Zhang *et al*. 2015), t_1 is pre-mixing temperature of HC(℃), and t_2 is temperature after mixing of heat carriers (℃).

The average evaporative heat consumption was calculated by Eq. 5,

$$E = \frac{c_1m_1(t_1-t_2)}{m_2x} \quad (5)$$

where E is the average evaporative heat consumption (MJ/kg).

RESULTS AND DISCUSSION

The DSC sample thermal analysis curve was obtained by subtracting the baseline of measurement without sample from the sample heat flow, and the results are shown in Figs. 3 and 4. The specific heat capacity of biomass ash was tested by the sapphire method, and a platinum crucible with a top cover was selected to shield the effect of thermal radiation. The results are shown in Fig. 5.

As shown in Fig. 3, biomass ash had three mass reduction stages at 35 to 1000 °C. The weight loss extremes were at 350 °C, 737°C, and 1100 °C. Contributions to weight loss correspond to the evaporation of water, the decomposition of K_2O (350 to 400 °C) to K_2O_2 and K (Duan *et al*. 2011), maximum weight loss corresponds to $Ca(OH)_2$ (500 to 600 °C) (Lin 2008), and the decomposition of $CaCO_3$ (750 °C) (Popescu *et al*. 2014), respectively. At 50 to 1000 °C the mass fraction of biomass ash decreased by 4.74%. After

1126 °C the weight loss corresponded to the melting of $AlKO_8Si_3$, $NaAlSi_3O_8$, and $CaMgSi_2O_7$ (Zhang *et al*. 2015). Figure 4 shows that the DSC signal of the biomass ash residue changed at 50 to 1200 °C, and the evaporation of water occurred within this temperature range. There was a clear exothermic peak at 740 °C, corresponding to the decomposition of $Ca(OH)_2$ and $CaCO_3$. Figure 5 shows that the specific heat of biomass ash under inert gas was approximately 0.83 to 1.48 J/(g•°C) at 50 to 1000 °C, which provides an important reference for the utilization of waste heat of biomass ash.

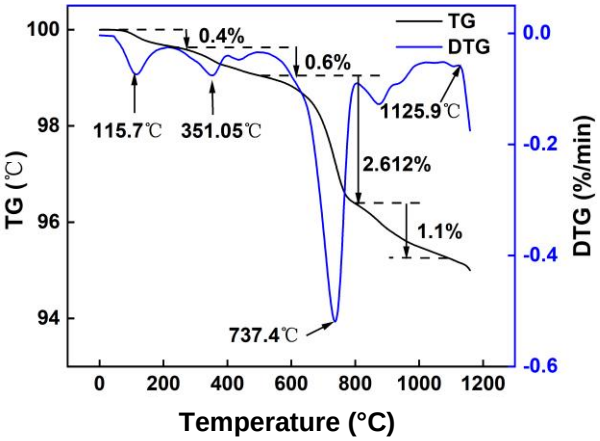

Fig. 3. TG-DTG of biomass ash

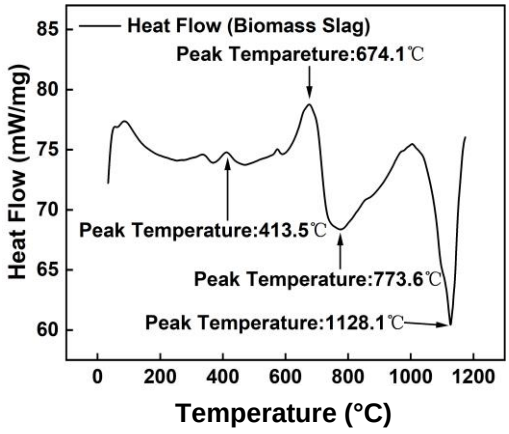

Fig. 4. DSC of biomass ash

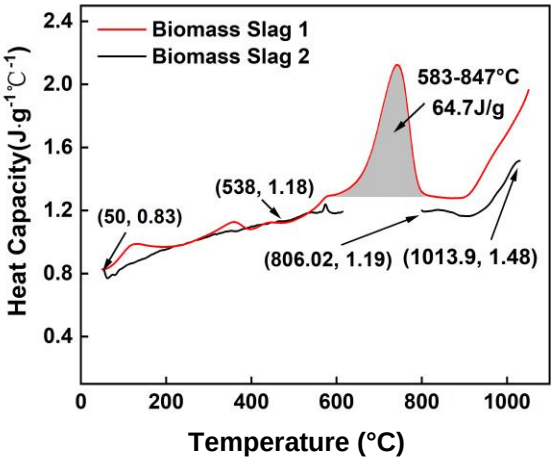

Fig. 5. Specific heat of biomass ash

Influence of D_{HC} and $MR_{HC/M}$ on Waste Heat Recovery Effect

The temperature of HC after recovering the waste heat from HTA is shown in Fig. 7, and the thermal efficiency of waste heat recovery was calculated according to the temperature change of biomass ash and HC as shown in Fig. 8.

Figure 6 shows the test of waste heat recovery from biomass ash by HC. The temperatures after waste heat recovery of 6, 9, 12, 15, and 18 mm D_{HC} were 401.8, 405.8, 399.4, 399, and 405.9 °C when the $MR_{HC/HC}$ to biomass ash was 1.5 and the T_{HTA} was 800 °C, respectively. The T_{HC} was in the range of 399 to 405.9 °C. With the change of the D_{HC}, there was a slight difference in the temperature after waste heat recovery, but it basically had no effect on the effect of waste heat recovery.

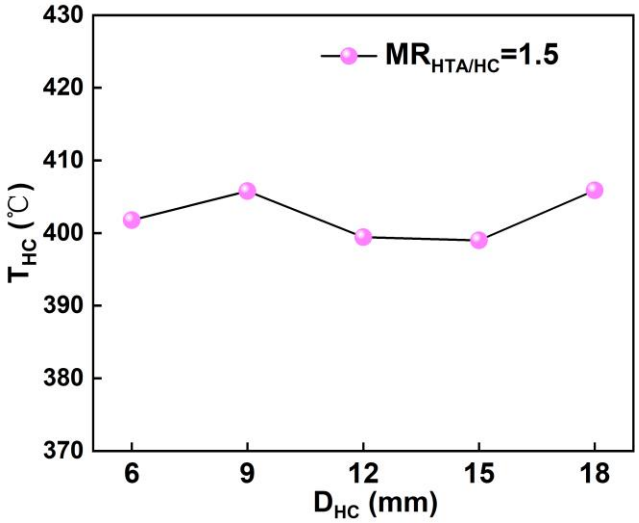

Fig. 6. Effect of diameter of heat carrier ball (D_{HC}) on the temperature of waste heat recovery

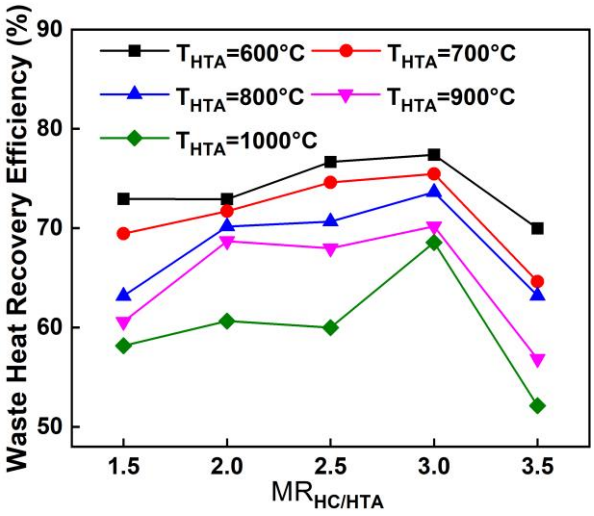

Fig. 7. Effect of mixing mass ratio of heat carrier and high temperature ash ($MR_{HC/HTA}$) and temperature of heat carrier (T_{HTA}) on mixing temperature

From Fig. 7, the influence of T_{HTA} and $MR_{HC/HTA}$ is obvious. Under the condition of constant mixed mass ratio, the T_{HC} increases with the increase of biomass ash temperature. At a constant biomass ash temperature, the carrier bulb temperature decreases with the increase of the carrier bulb mass; the decreasing trend becomes obvious at the $MR_{HC/HTA}$ of 2.5 to 3.

Figure 8 shows that the waste heat recovery efficiency decreased with the increase of temperature at a constant mixing mass ratio, and the highest waste heat recovery efficiency was achieved at a mixing mass ratio of 3 at a constant biomass ash temperature. The highest waste heat recovery efficiency was 77.4% when the temperature of biomass ash was 600 °C and the mixing mass ratio was 3.

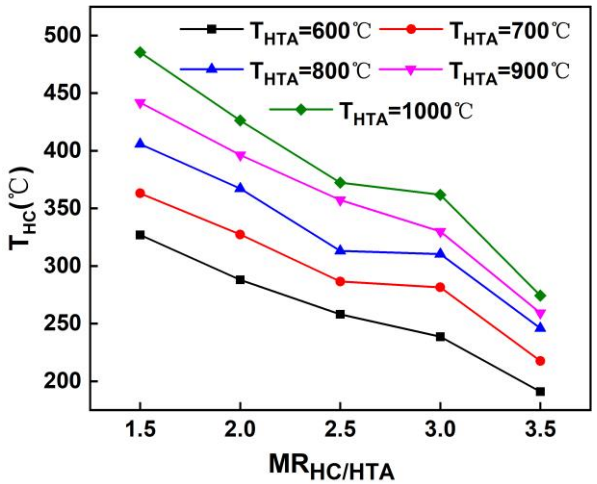

Fig. 8. Effect of mixing mass ratio of heat carrier and high temperature ash ($MR_{HC/HTA}$) on waste heat recovery efficiency

Effect of D_{HC} and mixing ratio on mixing and drying

The temperature of HC was recorded every 30 seconds, as shown in Fig. 9. The dehydration of biomass is shown in Fig. 10, and the drying thermal efficiency is shown in Fig. 11. The average evaporation energy consumption visually reflects the energy consumption of evaporating unit mass of water in the drying process, and the average evaporation energy consumption in the mixed drying process is shown in Fig. 12.

Figure 9 shows that the temperature of the HC entering the mixing and drying device after the temperature dropped faster above 150 °C. As the temperature of the HC dropped, the trend of temperature change was no longer obvious after 4.5 minutes. When entering the mixing dryer for a definite period of time, the temperature of the HC decreased more slowly as the particle size became larger, and the difference in temperature decrease became more and more obvious when the temperature decreased to below 150 °C. Therefore, stirring should be accelerated in the early stage of the mixing and drying process to make the mixing and heat exchange more adequate and avoid heat accumulation causing pyrolysis.

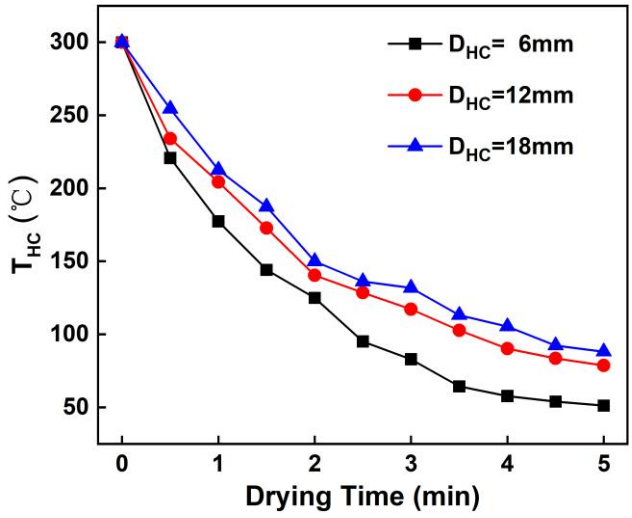

Fig. 9. Variation of temperature during the drying process of different D_{HC}

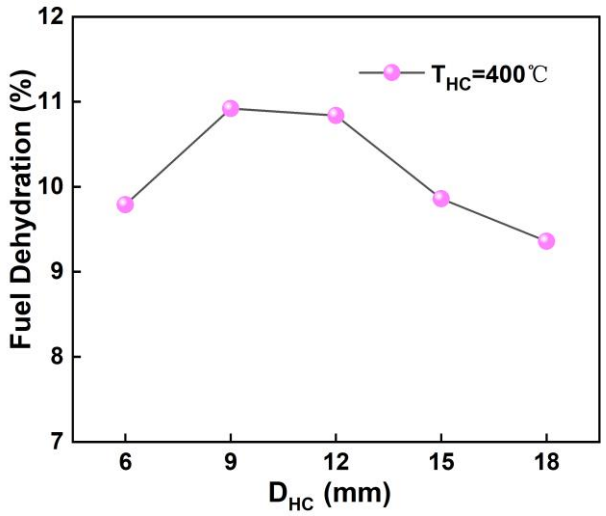

Fig. 10. Effect of D_{HC} on fuel dehydration percentage

From Fig. 10, it can be seen that when the D_{HC} was between 6 and 18 mm, the drying effect was best when the diameter of the carrier ball was 9 and 12 mm, and the fuel dehydration percentage was 10.92% and 10.84%, respectively. The fuel dehydration was less when the diameter of the carrier ball was 6 mm, which may be because the smaller diameter of the carrier ball exerts heat faster and more heat escapes to the environment.

Figure 11 shows that under the same carrier sphere temperature, as the mixed mass ratio increased, the biomass dehydration percentage also increased. After the mass of the carrier sphere increased, the heat input to the system increased, and the contact area between the biomass fuel and the carrier sphere increased, which was more favorable to the heat and moisture precipitation of biomass. When the temperature of the HC was constant, the dehydration of biomass increased significantly with the increase of the mass ratio of the HC. When the mixing ratio was constant, the mixed drying dehydration changed significantly when the carrier sphere temperature increased from 350 to 400 °C, which indicated that faster loss of moisture during drying was more significant when the

carrier sphere temperature increased in this temperature range. At a mixing ratio of 3 and a mixing temperature of 450 °C, the highest biomass dehydration percentage was 17.33%. At 300 to 450 °C, the increase of biomass dehydration percentage increased with the increase of mixing temperature at the same mixing ratio; however, at 450 to 500 °C and mixing ratio of 2, the biomass dehydration only increased from 12.99% to 13.37% and showed a decreasing trend at mixing ratios of 2.5 and 3. The dehydration percentage decreased from 15.76% at mixing ratio of 2.5 to 14.91%, and the dewatering decreased from 17.33% to 16.63% at the mixing ratio of 3. This indicates that heat accumulation occurred at the mixing temperature of 450 to 500 °C, and aerobic pyrolysis of a small amount of biomass consumed some heat, resulting in a decrease in the overall drying efficiency.

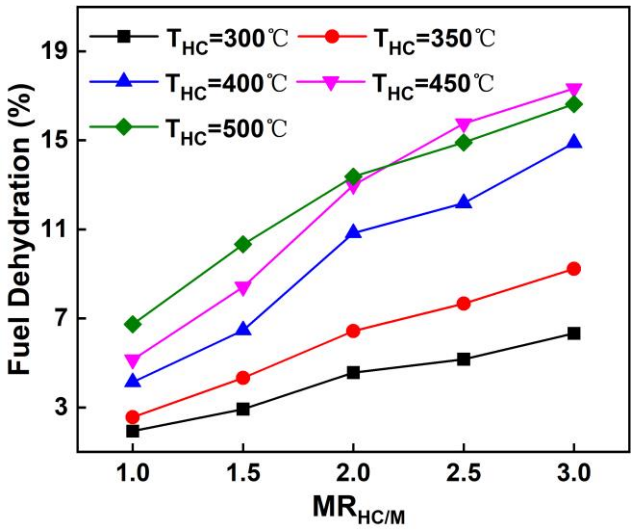

Fig. 11. Effect of $MR_{HC/M}$ on fuel dehydration percentage

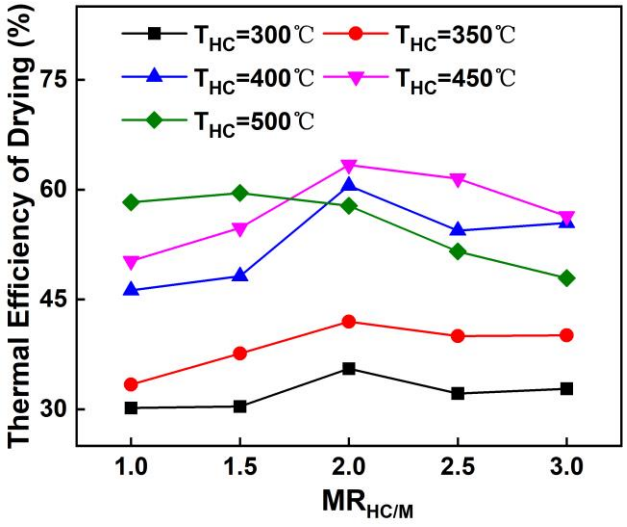

Fig. 12. Effect of mixing ratio on drying thermal efficiency

From Fig. 12, it can be seen that at 300 to 450 °C and with a mixing mass ratio of 1 to 3, when the mixing mass ratio was constant, the drying thermal efficiency increased with the increase of the HC temperature, and the growth trend was the largest at 350 to 400 °C; when the mixing temperature was constant, the drying thermal efficiency increased at the mixing mass ratio of 1 to 2, and the drying thermal efficiency decreased with the mixing mass ratio when the mixing ratio was greater than 2. The highest drying thermal efficiency was 63.39% when the mixing mass ratio was 2 and the temperature of the heat carrier was 450 °C. The drying thermal efficiency decreased significantly when the temperature of the HC was 500 °C and the mixing ratio increased from 1.5 to 3. There was partial pyrolysis of biomass caused by heat accumulation in the mixing and drying process under this mixing ratio. The thermal efficiency of hot air drying was 50 to 70%, the drying time was 20 to 40 min, and the tail gas temperature was above 100 °C (Haarlemmer 2015). By comparison, with hot air drying, the mixed drying did not need to recover the waste heat of the subsequent tail gas, and the drying time was only about 5 min.

Figure 13 shows that the average evaporation energy consumption was the lowest when the mixed mass ratio was 2 or close to 2 when the carrier sphere temperature was constant; when the mixed mass ratio was fixed, the average evaporation energy

consumption was lower at 400 to 450 °C; the average evaporation energy consumption was 3.73 MJ/Kg when the mixed mass ratio was 2 and the carrier sphere temperature was 400 °C, and the average evaporation energy consumption was 3.56 MJ/Kg. It follows that 400 to 450 °C is a suitable temperature parameter for mixing and drying. At 500 °C, with the increase of mixing ratio, the partial pyrolysis of high moisture biomass caused by the heat accumulation problem in the mixing process leads to the increase of average energy consumption in evaporation.

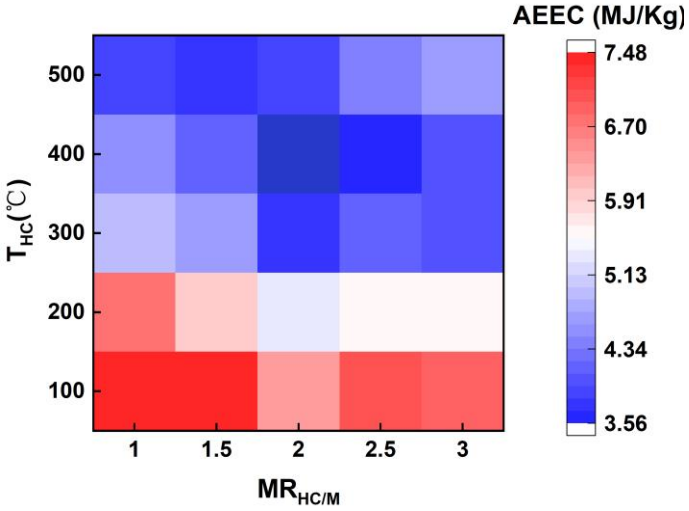

Fig. 13. Evaporation energy consumption (AEEC) per unit of moisture in the mixing and drying process ($MR_{HC/M}$)

CONCLUSIONS

1. The specific heat capacity of biomass ash at 35 to 1000 °C was measured by the sapphire method as 0.83 to 1.48 J/(g•°C).
2. In the process of recovering waste heat from biomass ash with heat carriers (HC), the diameter of the heat carrier (D_{HC}) had no effect on the efficiency after waste heat recovery. However, a larger value of D_{HC} will prolong the mixing and drying time.
3. The input heat source temperature and mass ratio are important factors affecting waste heat recovery and mixing and drying. When the HC temperature and mixing mass ratio are too high, it will reduce the thermal efficiency of drying.

REFERENCES CITED

Agar, D. A., Svanberg, M., Lindh, I., and Athanassiadis, D. (2020). "Surplus forest biomass – The cost of utilisation through optimised logistics and fuel upgrading in northern Sweden," *Journal of Cleaner Production* 275, article no. 123151. DOI: 10.1016/j.jclepro.2020.123151

Amos, W. A. (1998). *Report on Biomass Drying Technology*, U.S. Department of Energy, National Renewable Energy Lab, Golden, CO. DOI: 10.2172/9548

ASTM E-1269 (2011). "Standard test method for determining specific heat capacity by

differential scanning calorimetry," ASTM International, West Conshohocken, USA.

Das, B., Prakash, S., Reddy, P., and Misra, V. N. (2007). "An overview of utilization of slag and sludge from steel industries," *Resources, Conservation and Recycling* 50(1), 40-57. DOI: 10.1016/j.resconrec.2006.05.008

Duan, Y., Bo, Z., Dan, C. S., and Johnson, J. K. (2011) "CO_2 capture properties of M–C–O–H (M=Li, Na, K) systems: A combined density functional theory and lattice phonon dynamics study," *Journal of Solid State Chemistry* 184(2), 304-311. DOI: 10.1016/j.jssc.2010.12.005.

Fagernäs, L., Brammer, J., Wilen, C., Lauer, M., and Verhoeff, F. (2010). "Drying of biomass for second generation synfuel production," *Biomass and Bioenergy* 34(9), 1267-1277. DOI: 10.1016/j.biombioe.2010.04.005

Favero, A., Daigneault, A., and Sohngen, B. (2020). "Forests: Carbon sequestration, biomass energy, or both?," *Science Advances* 6(13), eaay6792. DOI: 10.1126/sciadv.aay6792

GB/T 28733(2012). "Solid biomass fuel full moisture determination method," Standardization Administration of China, Beijing, China.

Haarlemmer, G. (2015). "Simulation study of improved biomass drying efficiency for biomass gasification plants by integration of the water gas shift section in the drying process," *Biomass & Bioenergy* 81, 129-136. DOI: 10.1016/j.biombioe.2015.06.002

Holmberg, H. (2007). *Biofuel Drying as a Concept to Improve the Energy Efficiency of an Industrial CHP Plant*, Ph.D. Dissertation, Helsinki University of Technology, Helsinki, Finland.

Jahanshahi, S., Xie, D., Pan, Y., Ridgeway, P., and Mathieson, J. (2011). "Dry slag granulation with integrated heat recovery," in: *1st International Conference on Energy Efficiency and CO_2 Reduction in the Steel Industry*, Dusseldorf, Germany.

Junxiang, L., Qingbo, Y., Jiayan, P., Xianzhong, H., and Wenjun, D. (2015). "Thermal energy recovery from high-temperature blast furnace slag particles," *International Communications in Heat and Mass Transfer* 69, 23-28. DOI: 10.1016/j.icheatmasstransfer.2015.10.013

Li, B., Chen, H., Ju, F., Yang, H., and Zhang, S. (2011). "Study of hot air drying characteristics of biomass fluidized bed," *Taiyangneng Xuebao/Acta Energiae Solaris Sinica* (06),782-786. DOI:CNKI:SUN:TYLX.0.2011-06-003

Lin, H. (2008). *Research on Superficial Modification of Calcium Hydroxide and its Application*, Master's Thesis, Guangdong University of Technology, Guangzhou, China.

Munawar, M. A., Khoja, A. H., Naqvi, S. R., Mehran, M. T., Hassan, M., Liaquat, R., and Dawood, U. F. (2021). "Challenges and opportunities in biomass ash management and its utilization in novel applications," *Renewable and Sustainable Energy Reviews* 150, article no. 111451. DOI: 10.1016/j.rser.2021.111451

National Energy Administration (2021). "The National Energy Administration held a press conference to introduce the energy and economic situation in the first half of 2021," (http://www.nea.gov.cn/2021-07/29/c_1310093667.htm), Accessed 29 July 2021.

Popescu, M. A., Isopescu, R., Matei, C., Fagarasan, G., and Plesu, V. (2014). "Thermal decomposition of calcium carbonate polymorphs precipitated in the presence of ammonia and alkylamines," *Advanced Powder Technology* 25(2), 500-507. DOI:10.1016/j.apt.2013.08.003

Rupar, K., and Sanati, M. (2003). "The release of organic compounds during biomass

drying depends upon the feedstock and/or altering drying heating medium," *Biomass and Bioenergy* 25(6), 615-622. DOI: 10.1016/S0961-9534(03)00055-2

Salomonsson, P. (2006). *Utvärdering av biobränsletorkanläggning på Borås Energi AB (Evaluation of the Biomass Dryer Plant on Borås Energi AB)*, Master's Thesis, Lund University, Lund, Sweden.

Seebold, S., Eberhard, M., Wu, G., Yazhenskikh, E., Sergeev, D., Kolb, T., and Müller, M. (2017). "Thermophysical and chemical properties of bioliq slags," *Fuel* 197, 596-604. DOI: 10.1016/j.fuel.2017.02.027

Shanmukharadhya, K., S., and Sudhakar, K., G. (2007). "Effect of fuel moisture on combustion in a bagasse fired furnace," *Journal of Energy Resources Technology* 129(3), 248-253. DOI: 10.1115/1.2748816

Smith, A. M. S., Tinkham, W. T., Roy, D. P., Boschetti, L., Kremens, R. L., Kumar, S. S., Sparks, A. M., and Falkowski, M. J. (2013). "Quantification of fuel moisture effects on biomass consumed derived from fire radiative energy retrievals," *Geophysical Research Letters* 40(23), 6298-6302. DOI: 10.1002/2013gl058232

Sunil K. T., Jayalaxmi D., Y. R. M., Gajanan K., Atanu R. P., and Lev O. F. (2020). "Utilisation perspective on water quenched and air-cooled blast furnace slags," *Journal of Cleaner Production* 262, article no. 121354. DOI: 10.1016/j.jclepro.2020.121354

Wei, C., Wu, L. B., Debo, L., Dingqing, L., and Yongxin, F. (2017). "Research and engineering application of heat recovery system for biomass boiler slag," *Guangdong Electric Power* 30(11), 12-16. DOI: 10.3969/j.issn.1007-290x.2017.011.003

Xing, X., Wang, R., Bauer, N., Ciais, P., and Xu, S. (2021). "Spatially explicit analysis identifies significant potential for bioenergy with carbon capture and storage in China," *Nature Communications* 12(1). DOI: 10.1038/s41467-021-23282-x

Zhang, L. M., Dong, X. G., Liu, K., Tan, H. Z., Wang, X. B., and Wei, B. (2015). "Effects of kaolin on slagging characteristics and mineral evolution of Zhongdong coal," *Journal of Fuel Chemistry* 43(10), 1176-1181.DOI: 10.11949/j.issn.0438-1157.20180751

Article submitted: February 12, 2022; Peer review completed: May 7, 2022; Revised version received and accepted: May 23, 2022; Published: July 26, 2022.
DOI: 10.15376/biores.17.3.5243-5254